Computers, Materials & Continua CMC, vol.63, no.1, pp.263-281, 2020

Reliability Analysis of Slope Stability Considering Temporal Variations of Rock Mass Properties

Xin Gu[2], Lin Wang[1, 2, 3], Fuyong Chen[2], Hongrui Li[2] and Wengang Zhang[1, 2, 3, *]

Abstract: Temporal variation of rock mass properties, especially the strength degradation due to drying-wetting cycles as well as the acidic wetting fluid (rainfall or reservoir water) is crucial to stability of reservoir rock slopes. Based on a series of drying-wetting cycling and experiments considering the influences of pH values, the degradation degree models of the reduced cohesion c', friction angle φ' are developed. 2D stability analysis of the slope is subsequently carried out to calculate the factor of safety (Fs) via limit equilibrium method (LEM) and a predictive model of Fs is built using multivariate adaptive regression splines (MARS), revealing the effect of the drying-wetting cycles and pH value. The reliability analysis by Monte Carlo simulation is performed to rationally consider the uncertainty and the temporal variation of the shear strength parameters of rock mass. Results indicate that the MARS-based model can estimate the Fs accurately. The Fs and the reliability index β decrease with increase of drying-wetting cycles, and the temporal variation of rock mass properties has significant influence on the slope reliability. Overlooking the temporal variation of rock properties may overestimate the Fs and reliability index β in the longer term.

Keywords: Reservoir slope stability, pH value, reliability analysis, temporal variation, strength degradation.

1 Introduction

The rock slope failure generally results in serious disasters, great property losses and casualties. The early studies on slope stability could be traced back to the 1970s [Matsuo and Kuroda (1974); Tang, Yucemen and Ang (1976)]. Recently, with the completion of Three Gorges Reservoir (TGR) Project, the reservoir rock slope stability assessment has attracted increasing attentions in geotechnical and geological engineering throughout the world. The reservoir water levels rise and fall repeatedly within 145-175 m levels all year round, as a result of which the rock-soil mass in the hydro-fluctuation zone of the

[1] Key Laboratory of New Technology for Construction of Cities in Mountain Area, Chongqing University, Chongqing, China.

[2] School of Civil Engineering, Chongqing University, Chongqing, China.

[3] National Joint Engineering Research Center of Geohazards Prevention in the Reservoir Areas, Chongqing University, Chongqing, China.

[*] Corresponding Author: Wengang Zhang. Email: zhangwg@cqu.edu.cn; zhangwg@ntu.edu.sg.

Received: 01 June 2019; Accepted: 21 June 2019.

reservoir area will experience the alternation of drying-wetting cycles once or several times a year. Liu et al. [Liu, Zhang and Fu (2014)] demonstrated that the temporal variation of the shear strength parameters exists in argillaceous sandstones and the acidic environment can accelerate the damage or the degradation of the rock-soil mass properties with time.

Numerical methods are a good substitute to study the slope stability, which are more cost-effective than experiments and can provide physical perceptions difficult to obtain via 'pure' experiments [Zhou, Zhuang, Zhu et al. (2018); Zhou, Zhuang and Rabczuk (2019, 2018a); Zhou, Rabczuk and Zhuang (2018b)]. To provide a relatively accurate estimation of slope stability, lots of attempts have been made to develop the deterministic computational models to evaluate slope stability using numerical methods [Merifield, Lyamin and Sloan (2006); Li, Lyamin and Merifield (2009); Shen and Karakus (2013)] and simplified analytical approaches, such as the limit equilibrium method (LEM) [Sun, Zhao, Shang et al. (2012); Zhao, Tong and Lü (2014)] as well as the limit analysis theory [Viratjandr and Michalowski (2006); Drescher and Michalowski (2009); Yang and Pan (2015); Pan, Xu and Dias (2017)]. The deterministic analysis with the factor of safety (Fs) is commonly utilized to evaluate the slope stability. The rock slope is assumed to be homogeneous and rock mass properties are selected to be of representative values to calculate the Fs in deterministic analysis. This may not be the real condition in geotechnical engineering. And many studies have shown that the factor of safety cannot fully evaluate the stability of slope since some slopes with a high factor of safety still ultimately fail [Zhang, Wang, Huang et al. (2017); Oguz, Yalcin and Huvaj (2017); Liu and Cheng (2018)]. Furthermore, there are uncertainty and inherent variability in the rock mass. Reliability analysis is usually required for rock slope engineering [Griffiths, Huang and Fenton (2009); Phoon and Kulhawy (1999a, 1999b); Ghasemi, Brighenti, Zhuang et al. (2015); Zhang and Goh (2018)] and the probabilistic assessment [Ghasemi, Rafiee, Zhuang et al. (2014)] is conducted through Monte Carlo simulation [Park, West and Woo (2005); Li, Cassidy, Wang et al. (2012); Johari, Momeni and Javadi (2015)]. In addition, the spatial variability of rock-soil mass is usually considered in the slope stability analysis [Cho (2007); Li, Wang, Cao et al. (2013); Liu, Wang and Li (2019)]. However, the temporal variation of the shear strength parameters for rock mass properties is seldom taken into consideration, which has significant influence on the slope stability. Furthermore, few literatures have reported the reliability analysis on the slope stability simultaneously considering the effect of the temporal variation of the shear strength parameters and the pH value of the acidic environment. Thus, how to rationally consider the temporal variation of rock properties and the pH value of the acidic environment in the reliability analysis of slope stability remains a challenging task.

This study intends to investigate the effect of the temporal variation of rock properties on the reliability analysis of slope stability. Firstly, the fitting formulas of the degradation degree of the reduced cohesion c', friction angle φ' in the rock mass are established on the basic of the experimental results by Liu et al. [Liu, Zhang and Fu (2014)]. Then, a deterministic analysis is carried out to explore the effects of the pH value and drying-wetting cycles on the safety factor (Fs) of the slope. Next, a predictive model based on multivariate adaptive regression splines (MARS) is developed to relate the factor of

safety (Fs) to pH value and the drying-wetting cycles *N*. Afterwards, the influences of the coefficient of variations of cohesion and friction angle (COV_c and COV_φ) on the reliability index β of reservoir rock slope are investigated, followed by the analysis on the impacts of the pH value, the drying-wetting cycles and the correlation coefficient $\rho_{c,\varphi}$. Comparisons are also made to investigate the effect of these influential factors on the stability of the argillaceous sandstone slope. The obtained results of this paper can provide reference for theoretical analysis and practical application of slope stability in the field of water-rock interaction and related fields under acidic environment.

2 Numerical model of slope

Numerical Software Slide2 [Rocscience Inc (2018)] is adopted to carry out the reliability analysis of slope stability. The prototype slope illustrated in Fig. 1 is based on the study by Xiao et al. [Xiao, Guo and Zeng (2017)], with slope angle of 27°, width of 60 m, height of 10 m, and constant unit weight of 24 kN/m^3.

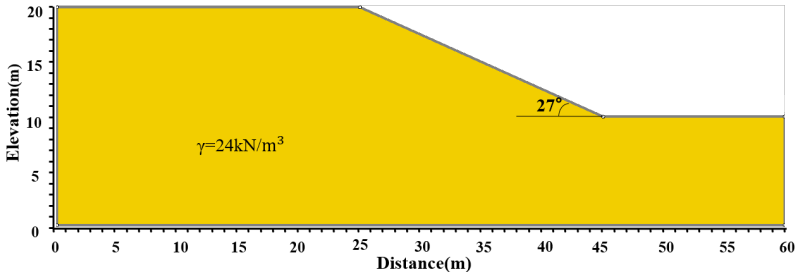

Figure 1: Geometry of the slope

Based on the results by Liu et al. [Liu, Zhang and Fu (2014)], a drying-wetting cycle last for one day and the values of cohesion *c*, friction angle φ of the argillaceous sandstone at different drying-wetting cycles can be obtained. Tabs. 1, 2 and 3 show values of *c*, φ with different drying-wetting cycles for three typical pH values. The factor of safety for slope of the same dimension as that in Fig. 1 analyzed by Xiao et al. [Xiao, Guo and Zeng (2017)] is calculated by Bishop's simplified method [Bishop (1955)], based on the mean value of shear strength parameters. The obtained value is 0.987, almost equal to 0.988 that computed by the Software Slide2. Therefore, the slope numerical model in Fig. 1 has been validated to be appropriate to conduct the following analysis.

Table 1: Strength degradation with drying-wetting cycles for pH=7

Cycles	*c* (MPa)	φ (°)	c'(kPa)	φ'(°)
0	10.07	45.14	170.41	38.37
5	5.35	33.02	90.46	28.06
10	4.79	31.36	81.00	26.65
15	4.44	30.33	75.18	25.78
20	4.19	29.58	70.93	25.14

30	3.83	28.49	64.77	24.21
40	3.56	27.69	60.28	23.54
45	3.45	27.36	58.41	23.25
50	3.35	27.06	56.73	23.00
100	2.68	25.04	45.38	21.28
150	2.28	23.82	38.51	20.25
200	1.98	22.94	33.54	19.50
250	1.75	22.24	29.63	18.91
300	1.56	21.67	26.41	18.42
350	1.40	21.18	23.66	18.00
400	1.26	20.76	21.26	17.64
450	1.13	20.38	19.13	17.32
500	1.02	20.04	17.22	17.03
550	0.91	19.73	15.48	16.77
600	0.82	19.45	13.89	16.53
650	0.73	19.19	12.42	16.31
700	0.65	18.95	11.06	16.11
750	0.58	18.72	9.78	15.91
800	0.51	18.51	8.59	15.73
850	0.44	18.31	7.46	15.56

Table 2: Strength degradation with drying-wetting cycles for pH=5

Cycles	c (MPa)	φ (°)	c'(kPa)	φ'(°)
0	10.07	45.14	170.41	38.37
5	5.13	32.86	86.82	27.93
10	4.58	30.76	77.55	26.15
15	4.25	29.45	71.86	25.04
20	4.00	28.49	67.71	24.22
30	3.65	27.09	61.69	23.03
40	3.39	26.07	57.32	22.16
45	3.28	25.65	55.50	21.80
50	3.18	25.26	53.86	21.47
100	2.53	22.68	42.80	19.27
150	2.13	21.11	36.11	17.95
200	1.85	19.98	31.27	16.99
250	1.62	19.10	27.47	16.23
300	1.44	18.37	24.33	15.61

350	1.28	17.75	21.65	15.09
400	1.14	17.21	19.32	14.63
450	1.02	16.73	17.25	14.22
500	0.91	16.30	15.39	13.85
550	0.81	15.91	13.70	13.52
600	0.72	15.55	12.15	13.22
650	0.63	15.22	10.71	12.94

Table 3: Strength degradation with drying-wetting cycles for pH=3

Cycles	c (MPa)	φ (°)	c'(kPa)	φ'(°)
0	10.07	45.14	170.41	38.37
5	4.08	30.77	69.09	26.15
10	3.02	28.04	51.16	23.84
15	2.36	26.34	39.99	22.39
20	1.88	25.09	31.77	21.33
30	1.17	23.27	19.82	19.78
40	0.66	21.94	11.09	18.65
45	0.44	21.38	7.46	18.18
50	0.25	20.89	4.19	17.75

In rock slope stability analysis, rock mass shear strength parameters are the most important index. Based on the intact rock strength, the strength of the rock mass can be derived via the Fesinke method [Zhou, Liu, Shang et al. (2012)], as shown in Eqs. (1)-(3).

$$c' = c \times I \tag{1}$$

$$I = \frac{1}{1+aIn\frac{H}{L}} \tag{2}$$

$$\varphi' = \varphi \times 0.85 \tag{3}$$

where c, φ is cohesion, friction angle of the intact rock. c', φ' are the reduced cohesion, friction angle of the rock mass and I is the reduction coefficient. a is the characteristic coefficient determined by the strength of the rock and the distribution of the structural plane of the rock mass. H is the height of slope while L is discontinuities spacing, both in meters. The derived strength parameters are listed in Tabs. 1, 2 and 3. Based on the values in these tables, the degradation degree for the rock mass can be calculated, the fitting formulas for which are determined by MATLAB program, with expressions presented in Tabs. 4 and 5. The fitting curves for degradation degree of cohesion c', friction angle φ' are plotted in Fig. 2.

Table 4: Degradation degree fitting formulas (%) for cohesion c'

pH	Fitting formulas (%)
7	y=9.695ln(x+0.04786)+29.480 R^2=0.9993
5	y=9.329ln(x+0.03083)+32.551 R^2=0.9994
3	y=16.528ln(x+0.1529)+32.221 R^2=0.9996

where y is the degradation degree of the reduced cohesion c', and x is the number of drying-wetting cycles.

Table 5: Degradation degree fitting formulas (%) for friction angle φ'

pH	Fitting formulas (%)
7	y=6.503ln(x+0.09875)+15.080 R^2=0.9992
5	y=8.251ln(x+0.2277)+12.260 R^2=0.9992
3	y=9.658ln(x+0.1991)+15.600 R^2=0.9999

where y is the degradation degree of the reduced friction angle φ', and x is the number of drying-wetting cycles.

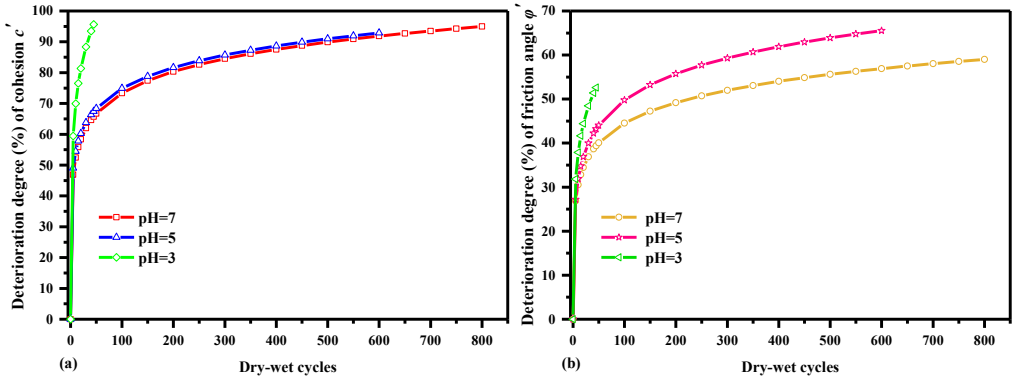

Figure 2: Degradation degree fitting curves for: (a) cohesion c', (b) friction angle φ'

It is obvious that the degradation degree of the reduced cohesion c', friction angle φ' increases with the drying-wetting cycles, in the pattern of logarithmic function. The degradation degree of the strength parameters in argillaceous sandstone slopes at specific drying-wetting cycles can be easily determined through the fitting formulas.

3 Rock slope stability analysis

3.1 Traditional deterministic analysis

To carry out the probabilistic analysis in this study, preliminary deterministic analysis has been implemented assuming a homogeneous rock slope. The factor of safety (Fs) is commonly utilized in traditional slope stability. The values of pH and drying-wetting cycles are considered when calculating the slope factor of safety. For the slope illustrated

in Fig. 1, the Fs values can be obtained via the limit equilibrium method (i.e., Simplified Bishop Method in this context) to give the data in Tab. 6. The plots in Fig. 3 indicate that the effects of the pH value and drying-wetting cycles on slope safety factor are significant.

Table 6: Fs values when for different pH values

Cycles \ pH	7	5	3
0	7.534	7.534	7.534
5	4.367	4.248	3.592
10	3.985	3.848	2.895
15	3.751	3.603	2.454
20	3.581	3.424	2.131
30	3.334	3.166	1.646
40	3.156	2.979	1.270
45	3.081	2.902	1.101
50	3.014	2.832	-
100	2.561	2.363	-
150	2.284	2.078	-
200	2.083	1.872	-
250	1.926	1.709	-
300	1.796	1.576	-
350	1.681	1.462	-
400	1.582	1.361	-
450	1.493	1.271	-
500	1.414	1.189	-
550	1.341	1.116	-
600	1.272	1.048	-
650	1.208	-	-
700	1.147	-	-
750	1.088	-	-
800	1.034	-	-

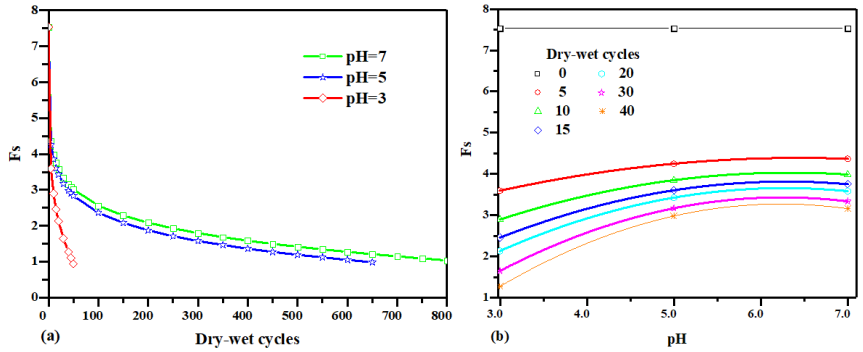

Figure 3: Effect of pH and dry-wet cycles on the safety factor (Fs) of slope

As shown in Fig. 3(a), the factor of safety decreases continuously with the number of drying-wetting cycles. For instance, the factor of safety decreases from 7.534 to 1.034 after 800 cycles when pH=7 while Fs decreases from 7.534 to 1.048 after 600 cycles when pH=5. By contrast, Fs decreases from 7.534 to 1.101 after 45 cycles when pH=3. Obviously, the lower the pH value is, the fewer cycles the slope can sustain before an impending failure. For simplicity, Fig. 3(b) only plots the results of the first 40 cycles as an example to illustrate the effect of the pH value on the factor of safety (Fs). In the process of gradual decrease of pH, the significant change appears in the influence of pH on the factor of safety of slope stability at any cycle, and this influential zone occurs between pH=3.0 and pH=5.0 (Fig. 2(b)), indicating that the Fs of argillaceous sandstone slope is sensitive to the pH value within this range. By contrast, the pH value between 5.0 and 7.0 has less significant impact on Fs for the argillaceous sandstone slope.

3.2 Influence of temporal variation of rock properties

As mentioned above, the drying-wetting cycles and the pH values will accelerate the shear strength degradation. However, few efforts have been made to systematically reveal the effect of this type of temporal variation of rock properties on the slope stability in the previous researches. Thus, this section intends to deal with this problem based on the calculated results from the Software Slide2. To show how the safety factors (Fs) of slip surfaces at various depths change with drying-wetting cycles in different pH values and to approximately estimate the Fs of the slip surface at certain depth, twelve typical plots of Fs as well as the slip surfaces after different drying-wetting cycles are shown in Fig. 4. In Fig. 4, the label is filled with different colors from top to bottom. And blue elements represent high Fs values while red elements correspond to low Fs values.

Without considering the temporal variation of rock mass properties, the Fs value will keep constant at 7.534. After comparison among these twelve trend charts, it is worth noting that the safety factors of the slip surfaces at the same depth decrease with the drying-wetting cycles in three typical pH values, which reveals a pattern of degradation of Fs. In the early period of the drying-wetting cycling, the slip surfaces with various Fs values at different depths display several layers with different colors, such as in Figs. 4(b), 4(c) and 4(f). As shown in Figs. 4(b), 4(c) and 4(d), the scale of the slip surfaces with low Fs values becomes bigger and bigger with the increase of the drying-wetting cycles with the passage of time.

And in Figs. 4(f), 4(g) and 4(h) (or Figs. 4(j), 4(k) and 4(l)), there exist the similar phenomena.

Therefore, the temporal variation of rock mass properties has significant influence on the safety factor (Fs) of the slopes, and it cannot be overlooked in the stability analysis of the reservoir rock slopes.

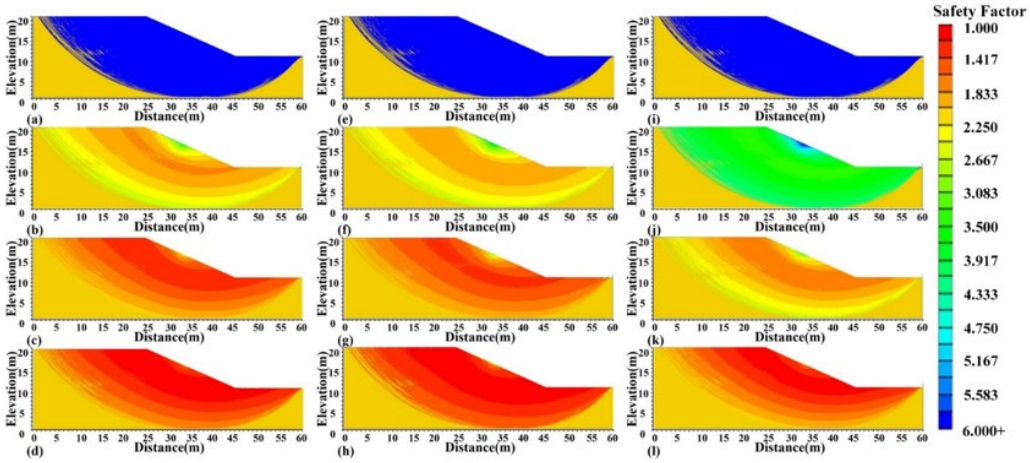

Figure 4: Fs of the slip surfaces at various depths in different drying-wetting cycles for pH=3.0, 5.0, 7.0, respectively. (a) 0 cycles in pH=7.0; (b) 300 cycles in pH=7.0; (c) 600 cycles in pH=7.0; (d) 800 cycles in pH=7.0; (e) 0 cycles in pH=5.0; (f) 200 cycles in pH=5.0; (g) 400 cycles in pH=5.0; (h) 600 cycles in pH=5.0; (i) 0 cycles in pH=3.0; (j) 10 cycles in pH=3.0; (k) 30 cycles in pH=3.0; (l) 45 cycles in pH=3.0

4 MARS-based approach for further slope stability analysis

To better understand the effect of pH value and drying-wetting cycles on the safety factor (Fs), multivariate adaptive regression splines (MARS) are used in this section for the surrogate model development. MARS was first proposed by Friedman [Friedman (1991)], as a nonlinear and nonparametric regression methodology that approximate the relationship between the inputs and the outputs. And there is no need for MARS to explore the form of the numerical function in advance, which is similar with neural networks [Zhang and Goh (2016); Zhang, Goh, Zhang et al. (2015); Guo, Zhuang and Rabczuk (2019); Goh, Zhang, Wang et al. (2019)].

Let y be the target dependent responses and X=(X_1 ,..., X_P) be a vector of P input variables. Then it is hypothesized that the data are generated on the basic of an unknown "true" model. For a continuous response, this would be:

$$y = f(X_1, ., X_P) + e = f(X) + e \quad (4)$$

where e is the fitting error. f is the model built by MARS, being made up of basic functions (BFs) that are splines piecewise polynomial functions. For simplicity, only the piecewise linear function is considered in this context. And the piecewise linear functions are in the form of max(0, x-t).This means that only the positive part is utilized, otherwise the value zero will be given to it. The max(0, x-t) is defined as follows:

$$max(0, x-t) = \begin{cases} x-t, if\ x \geq t \\ 0, otherwise \end{cases} \quad (5)$$

Based on the MARS, the model f(x) can be defined as follows:

$$f(x) = a_0 + \sum_{i=1}^{M} a_i B_i(X) \quad (6)$$

where the coefficients a_i in Eq. (6) are constants, obtained by the least-squares method. And each $B_i(X)$ is a basic function or the combination of two or more spline functions (Higher orders can be utilized only when the data warrants it. For simplicity, at most second-order is adopted).

According to MARS, it is achieved by a two-phase process. The forward phase adds functions and finds potential knots to improve the performance, producing a complicated and overfit model. And the backward phase is used to prune the least effective BFs. Considering that a current model is with M basis functions, and the next pair is added to the model as follows:

$$\hat{a}_{M+1} B_m(X) max(0, x_j - t) + \hat{a}_{M+2} B_m(X) max(0, t - x_j) \quad (7)$$

where $\hat{a}_{M+1}$ and $\hat{a}_{M+2}$ are estimated by the methodology of the least-squares method and $B_m(X)$ is the formerly determined BF with $0 \leq m \leq M$. The process of adding BFs will not stop until the model reaches some maximum number, generally producing a purposely over-fitted model.

In order to minimize the number of terms, a process called backward deletion follows. The backward procedure optimizes the model by pruning the redundant basis functions which have the lowest contribution to the model until the best sub-model is found. Then, the optimal MARS model is regarded as the sub-model which has the smallest value of *GCV* (generalized cross-validation) [Zhang and Goh (2013); Zhang, Zhang and Goh (2017); Goh, Zhang, Zhang et al. (2018); Zhang, Zhang, Wang et al. (2019); Liu, Zhang, Cheng et al. (2019)]. For a training data set with *N* observations, *GCV* is computed as:

$$GCV = \frac{\frac{1}{N}\sum_{i=1}^{N} [y_i - f(x_i)]^2}{\left[1 - \frac{M + d \times \frac{M-1}{2}}{N}\right]^2} \quad (8)$$

where M is the number of basic functions; d is the penalizing parameter, according to Friedman [Friedman (1991)], it has a default value of 3; N is the number of observations, and $f(x_i)$ is the predictive values of the MARS model.

Based on the factor of safety (Fs) of the slope at different drying-wetting cycles considering the effect of the pH value, the MARS-based mathematical equation of Fs is expressed as:

$$y = \alpha_0 + \sum_{i=1}^{14} \alpha_i BF_i \quad (9)$$

where y denotes the factor of safety, the values of the coefficients for the equation above are shown in Tab. 7 and BF_i (i=1, 2, 3, ⋯, 14) are basic functions, the equations of which shown in Tab. 8 below. Fig. 5 shows the plot of the factor of safety estimated by using Eq. (9) *vs.* the 163 calculated Fs values through Software Slide2. Eq. (9) is reasonably accurate with a high coefficient of determination (R^2) of 0.9995. Therefore, it can be used to predict the Fs of the slope at certain drying-wetting cycles under a given pH value.

Table 7: The values of the coefficients α_i (i=0, 1, 2, ⋯, 14)

α_0=2.9812	α_5=0.0012524	α_{10}=0.016175
α_1=-0.019265	α_6=-0.00022054	α_{11}=0.02834
α_2=0.031586	α_7=0.010639	α_{12}=0.0030972
α_3=0.11263	α_8=0.0067142	α_{13}=0.007013
α_4=-2.350	α_9=0.0010677	α_{14}=0.0010591

Table 8: The basic functions and corresponding equations of MARS model

BF1=*max*(0, X_1-20)	BF6=BF5×*max*(0, X_2-5)	BF11=*max*(0, 15-X_1)
BF2=*max*(0, 20-X_1)	BF7=BF5×*max*(0, 5-X_2)	BF12=*max*(0, X_1-1200)
BF3=*max*(0, X_2-5)	BF8=*max*(0, X_1-60)	BF13=*max*(0, X_1-40)
BF4=*max*(0, 5-X_2)	BF9=*max*(0, X_1-400)	BF14=*max*(0, 240-X_1)
BF5=*max*(0, 180-X_1)	BF10=BF4×*max*(0, 15-X_1)	

where X_1 denotes the number of drying-wetting cycles, and X_2 denotes the pH value.

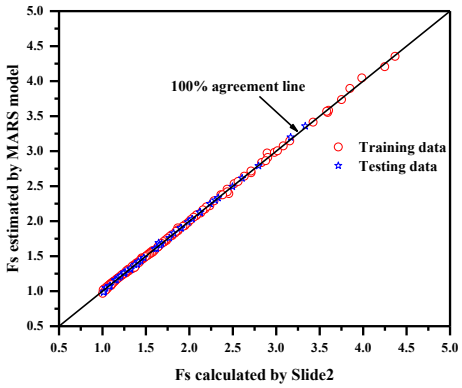

Figure 5: Predicted factor of safety Fs_{MARS} versus the calculated Fs_{Slide2}

5 Reliability analysis of rock slope stability

There exist uncertainty and temporal variations in the rock mass properties, which cannot be considered in the deterministic analysis in Section 3. Hence, a reliability-based approach is taken into consideration in this section to evaluate the reliability of rock slope stability. The cohesion and friction angle are assumed to be random variables. In this study, shear strength parameters are assumed to be characterized statistically by a normal distribution. In conventional analyses of slope reliability based on the LEM, the reliability index of slopes is generally calculated [Faravelli (1989); Duzgun, Yucemen and Karpuz (2003); Griffiths and Fenton (2004); Griffiths, Huang and Fenton (2009)] and the safety factor of the slope is utilized to calculate the integrated failure probability of the slope. When the factor of safety (Fs) equals to or greater than the unity, the slope is stable (safe), and when the factor of safety is less than 1.0, the slope is unstable (impending failure). Hence, the failure performance function of the slope is defined as follows:

$$G(i) = \begin{cases} 0, & Fs(i) \geq 1.0 \\ 1, & Fs(i) < 1.0 \end{cases} \tag{10}$$

where i =1, ⋯, N, and N is the number of the samples to be calculated.

Then, the failure probability and the reliability index [Ghasemi, Kerfriden, Bordas et al. (2015)] of the slope can be computed as follows:

$$P_f = \frac{1}{N}\sum_{i=1}^{N} G(i) \tag{11}$$

$$\beta = \Phi^{-1}\left(1 - P_f\right) \tag{12}$$

where Φ^{-1}(x) is the inverse function of the standard normal distribution function. Herein, a histogram of the factor of safety (Fs) in Fig. 6 is taken as an example to graphically illustrate the probability of failure (P_f), which is equal to the highlighted black area (FS<1) of the histogram divided by the total area of the histogram. And the statistics of the highlighted data are listed on the diagram. In this example, it reveals that 103/1000 points have a safety factor less than 1. This means the probability of failure equals 10.3%.

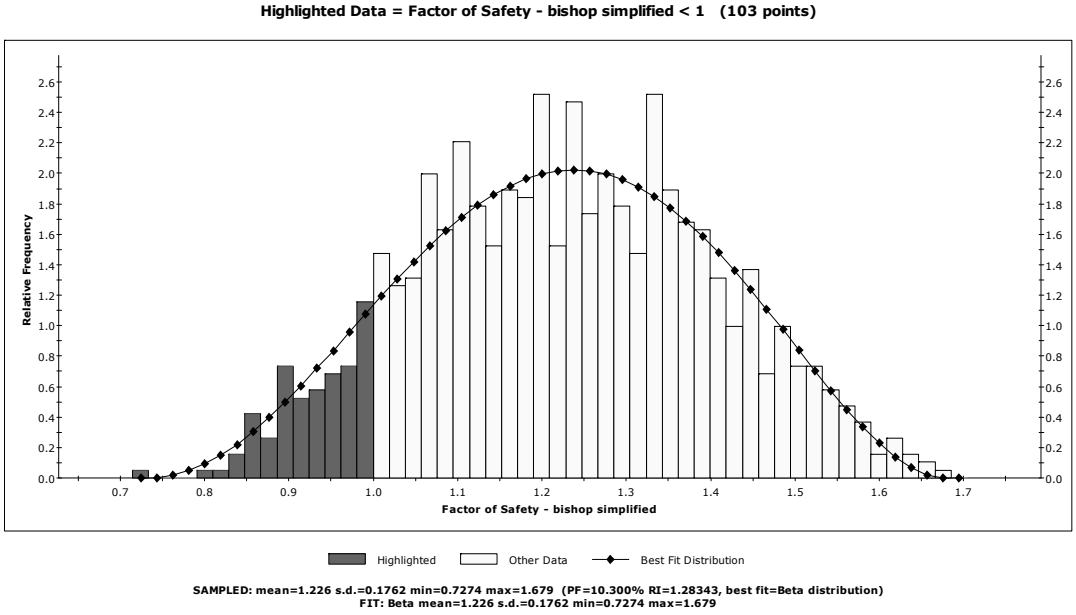

Figure 6: Histogram of the factor of safety (Fs)

In this section, three kinds of changing trends of COV_c and COV_φ are hypothesized (Tab. 9). Furthermore, different values of correlation coefficient $\rho_{c,\varphi}$ are also considered in the following ($\rho_{c,\varphi}$=-0.5, 0, 0.5). In the reliability analysis of slope stability, the analysis process is repeated until stable statistics of the outputs are obtained using 1000 Monte Carlo runs [Malkawi, Hassan and Sarma (2001); Park, West and Woo (2005); Li, Cassidy, Wang et al. (2012); Johari, Momeni and Javadi (2015)] to ensure that the calculated failure probability P_f can reach convergence.

Table 9: Three kinds of changing trends of COV_c and COV_φ

	Cycles / COV	0	10	20	30	40	45	50
Case 1	COV_c				0.3			
	COV_φ				0.1			
Case 2	COV_c	0.10	0.13	0.16	0.19	0.22	0.25	0.30
	COV_φ	0.05	0.06	0.07	0.075	0.08	0.09	0.10
Case 3	COV_c	0.10	0.13	0.16	0.19	0.22	0.25	0.30
	COV_φ	0.10	0.09	0.08	0.075	0.07	0.06	0.05

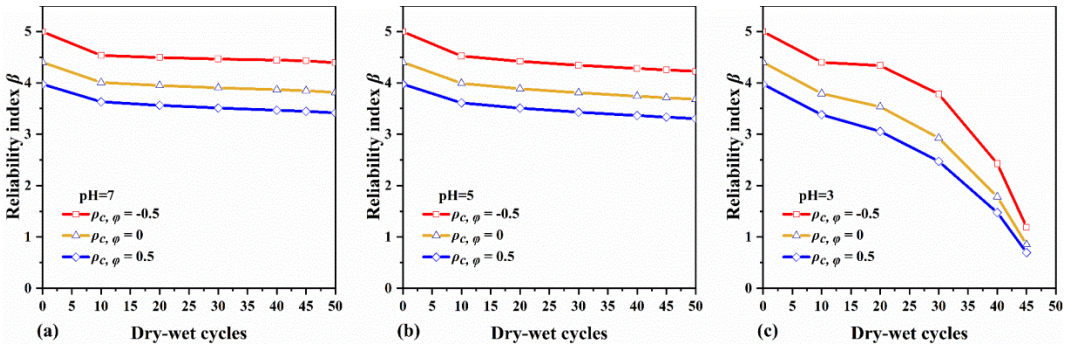

Figure 7: Effect of pH and correlation coefficient $\rho_{c,\varphi}$ on the reliability index of slope in Case 1

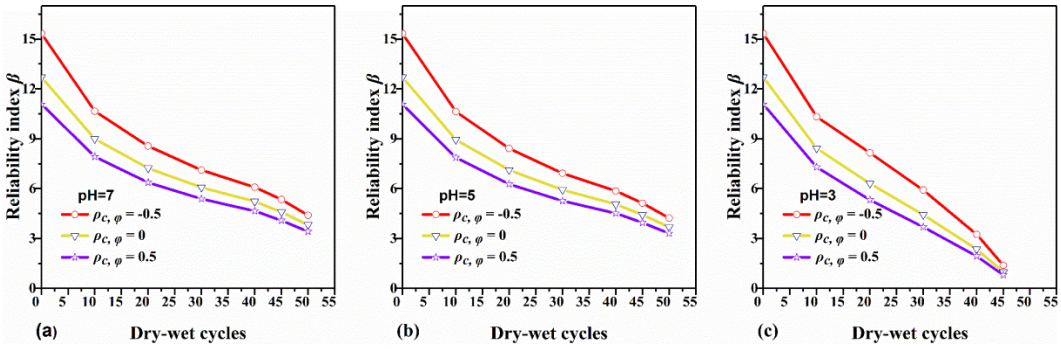

Figure 8: Effect of pH and correlation coefficient $\rho_{c,\varphi}$ on the reliability index of slope in Case 2

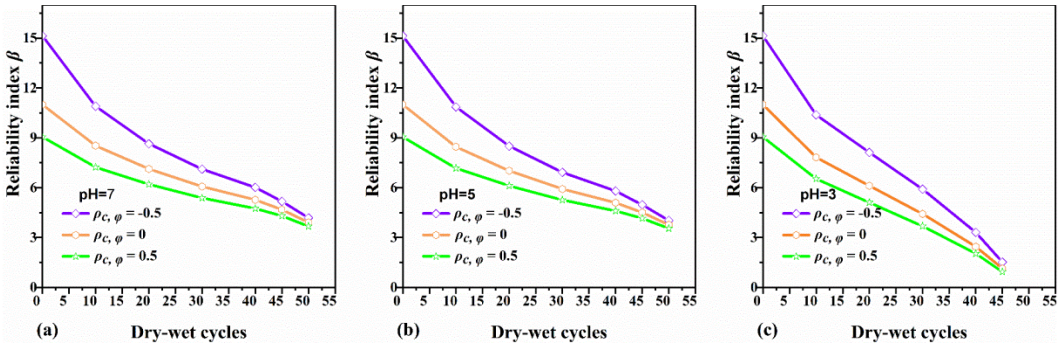

Figure 9: Effect of pH and correlation coefficient $\rho_{c,\varphi}$ on the reliability index of slope in Case 3

Figs. 7-9 illustrate the variation of the reliability index β with respect to various pH values and changing trends of COV_c, COV_φ, and these three cases all take the effect of the correlation coefficient $\rho_{c,\varphi}$ into consideration. Fig. 7 demonstrates the effect of the value of pH and correlation coefficient $\rho_{c,\varphi}$ on the reliability index of slope in Case 1 (Tab. 9), where $COV_c = 0.3$, $COV_\varphi = 0.1$. And Figs. 8 and 9 illustrate the influence of the pH value and correlation coefficient $\rho_{c,\varphi}$ on the reliability index of slope stability in Cases 2 and 3 (Tab. 9), respectively.

It can be seen from Figs. 7-9 that the reliability index β decreases with the drying-wetting cycles. And after the same cycle, the lower the value of pH is, the lower the reliability index β will be. According to Figs. 7(a) and 7(b), the reliability index β decreases only a bit in general. Fig. 7(c) shows that the reliability index β declines obviously with drying-wetting cycles. This phenomenon reveals that the reliability index β is less sensitive to the pH range of 5.0-7.0 than that from 3.0 to 5.0 when both COV_c and COV_φ keep constant. Also, the changing trend line of the reliability index β ($\rho_{c,\varphi}$=-0.5) almost parallels with that of the reliability index β (either $\rho_{c,\varphi}$=0 or $\rho_{c,\varphi}$=0.5). To some extent, this may be consistent with the results in Section 3.1 that the pH value from 5.0 to 7.0 has slighter effect on the Fs of the argillaceous sandstone slope compared to the pH value between 3.0 and 5.0.

According to Figs. 8 and 9 where COV_c and COV_φ change with the drying-wetting cycles, the difference between reliability index β at certain cycle seems to show opposite tendency towards the difference between COV_c and COV_φ. To be specific, however each of COV_c and COV_φ changes, as long as the difference between them gets greater, the difference in reliability index β of $\rho_{c,\varphi}$=-0.5, 0, 0.5 becomes less significant with the increase of the drying-wetting cycles.

Based on the analysis above, it can be concluded that the reliability index β is lower when the slope is in the acidic environment with a smaller pH value, which is consistent with the results in Section 3.1 in that the Fs of the argillaceous sandstone slope varies a lot in the pH value range of 3.0-5.0. It should also be noted that β declines with $\rho_{c,\varphi}$ changing from -0.5 to 0.5 when COV_c, COV_φ, the value of pH and drying-wetting cycles keep unchanged. It is well organized that reservoir water level fluctuation may affect the stability of reservoir rock slope. Although this study focuses on the temporal variation of

rock-mass properties on the slope stability, it can be extended to consider the effect of water level fluctuation by solving the corresponding partial differential equations of seepage modeling with the aid of advanced numerical methods [Ghasemi, Park and Rabczuk (2017); Ghasemi, Park and Rabczuk (2018)].

6 Summary and conclusions

In this study, both the deterministic and probabilistic analysis are conducted to explore the influence of the temporal variation of rock properties on the slope stability. A MARS-based predictive model is developed to relate Fs to the pH value and the drying-wetting cycles *N*. The following conclusions can be drawn from this study:

(1) The relationships among the pH value, drying-wetting cycles *N* and factor of safety (Fs) in temporally variable rocks can be well estimated using MARS. The proposed MARS-based predictive model is able to calculate the Fs accurately and efficiently.

(2) Both the Fs and the reliability index β decline with the decrease of the pH value. The Fs of the argillaceous sandstone slope is more sensitive to the pH value between 3.0 and 5.0 than that between 5.0 and 7.0. Hence, the pH value should be properly considered in the reservoir rock slope stability analysis.

(3) The spatial variations of rock properties (i.e., COV_c, COV_φ and the correlation coefficient $\rho_{c,\varphi}$) have significant effect on the reliability analysis of rock slope stability. And there exist different reliability index values in the slope with the same shear strength parameters when COV_c, COV_φ and $\rho_{c,\varphi}$ are different.

(4) Ignoring the temporal variation of rock properties may overestimate the Fs and the reliability index β of the rock slope. Therefore, the temporal variations of rock mass properties should be taken into consideration in the reliability analysis of rock slope stability.

Acknowledgement: The authors are grateful to the financial support from Natural Science Foundation of Chongqing, China (cstc2018jcyjAX0632), the Venture & Innovation Support Program for Chongqing Overseas Returnees (cx2017123), as well as Chongqing Engineering Research Center of Disaster Prevention & Control for Banks and Structures in Three Gorges Reservoir Area (SXAPGC18ZD01, SXAPGC18YB03). In addition, the authors would like to express their appreciation to Liu et al. [Liu, Zhang and Fu (2014)] for making their test results available for this work.

Conflicts of Interest: The authors declare that they have no conflicts of interest to report regarding the present study.

References

Bishop, A. W. (1955): The use of the slip circle in the stability analysis of slopes. *Geotechnique*, vol. 5, no. 1, pp. 7-17.

Cho, S. E. (2007): Effects of spatial variability of soil properties on slope stability. *Engineering Geology*, vol. 92, no. 3-4, pp. 97-109.

Drescher, A.; Michalowski, R. L. (2009): Three-dimensional stability of slopes and excavations. *Geotechnique*, vol. 59, no. 10, pp. 839-850.

Duzgun, H. S. B.; Yucemen, M. S.; Karpuz, C. (2003): A methodology for reliability-based design of rock slopes. *Rock Mechanics and Rock Engineering*, vol. 36, no. 2, pp. 95-120.

Faravelli, L. (1989): Response-surface approach for reliability analysis. *Journal of Engineering Mechanics*, vol. 115, no. 12, pp. 2763-2781.

Friedman, J. H. (1991): Multivariate adaptive regression splines. *Annals of Statistics*, vol. 19, no. 1, pp. 1-67.

Ghasemi, H.; Brighenti, R.; Zhuang, X.; Muthu, J.; Rabczuk, T. (2015): Optimal fiber content and distribution in fiber-reinforced solids using a reliability and NURBS based sequential optimization approach. *Structural and Multidisciplinary Optimization*, vol. 51, no. 1, pp. 99-112.

Ghasemi, H.; Kerfriden, P.; Bordas, S. P.; Muthu, J.; Zi, G. et al. (2015): Probabilistic multiconstraints optimization of cooling channels in ceramic matrix composites. *Composites Part B: Engineering*, vol. 81, pp. 107-119.

Ghasemi, H.; Park, H. S.; Rabczuk, T. (2017): A level-set based IGA formulation for topology optimization of flexoelectric materials. *Computer Methods in Applied Mechanics and Engineering*, vol. 313, pp. 239-258.

Ghasemi, H.; Park, H. S.; Rabczuk, T. (2018): A multi-material level set-based topology optimization of flexoelectric composites. *Computer Methods in Applied Mechanics and Engineering*, vol. 332, pp. 47-62.

Ghasemi, H.; Rafiee, R.; Zhuang, X.; Muthu, J.; Rabczuk, T. (2014): Uncertainties propagation in metamodel-based probabilistic optimization of CNT/polymer composite structure using stochastic multi-scale modeling. *Computational Materials Science*, vol. 85, pp. 295-305.

Goh, A. T. C.; Zhang, R. H.; Wang, W.; Wang, L.; Liu, H. L. et al. (2019): Numerical study of the effects of groundwater drawdown on ground settlement for excavation in residual soils. *Acta Geotechnica*.

Goh, A. T. C.; Zhang, W. G.; Zhang, Y. M.; Xiao, Y.; Xiang, Y. Z. (2016): Determination of EPB tunnel-related maximum surface settlement: a multivariate adaptive regression splines approach. *Bulletin of Engineering Geology and the Environment*, vol. 77, pp. 489-500.

Griffiths, D. V.; Fenton, G. A. (2004): Probabilistic slope stability analysis by finite elements. *Journal of Geotechnical and Geoenvironmental Engineering*, vol. 130, no. 5, pp. 507-518.

Griffiths, D. V.; Huang, J.; Fenton, G. A. (2009): Influence of spatial variability on slope reliability using 2-D random fields. *Journal of Geotechnical and Geoenvironmental Engineering*, vol. 135, no. 10, pp. 1367-1378.

Guo, H.; Zhuang, X.; Rabczuk, T. (2019): A deep collocation method for the bending analysis of kirchhoff plate. *Computers, Materials & Continua*, vol. 59, no. 2, pp. 433-456.

Johari, A.; Momeni, M.; Javadi, A. (2015): An analytical solution for reliability

assessment of pseudo-static stability of rock slopes using jointly distributed random variables method. *Iranlan Journal of Science and Technology-Transactions of Civli Engineering*, vol. 39, no. C2, pp. 351-363.

Li, A. J.; Cassidy, M. J.; Wang, Y.; Merifield, R. S.; Lyamin, A. V. (2012): Parametric Monte Carlo studies of rock slopes based on the Hoek-Brown failure criterion. *Computers and Geotechnics*, vol. 45, pp. 11-18.

Li, A. J.; Lyamin, A. V.; Merifield, R. S. (2009): Seismic rock slope stability charts based on limit analysis methods. *Computers and Geotechnics*, vol. 36, no. 1-2, pp. 135-148.

Li, L.; Wang, Y.; Cao, Z.; Chu, X. (2013): Risk de-aggregation and system reliability analysis of slope stability using representative slip surfaces. *Computers and Geotechnics*, vol. 53, pp. 95-105.

Liu, L. L.; Cheng, Y. M. (2018): System reliability analysis of soil slopes using an advanced kriging metamodel and Quasi-Monte Carlo simulation. *International Journal of Geomechanics*, vol. 18, no. 8.

Liu, L.; Zhang, S.; Cheng, Y. M.; Liang, L. (2019): Advanced reliability analysis of slopes in spatially variable soils using multivariate adaptive regression splines. *Geoscience Frontiers*, vol. 10, no. 2, pp. 671-682.

Liu, X. R.; Zhang, L.; Fu, Y. (2014): Experimental study of mechanical properties of argillaceous sandstone under wet and dry cycle in acid environment. *Rock and Soil Mechanics*, vol. 35, no. 2, pp. 45-52.

Liu, X.; Wang, Y.; Li, D. Q. (2019): Investigation of slope failure mode evolution during large deformation in spatially variable soils by random limit equilibrium and material point methods. *Computers and Geotechnics*, vol. 111, pp. 301-312.

Malkawi, A. I. H.; Hassan, W. F.; Sarma, S. K. (2001): Global search method for locating general slip surface using Monte Carlo techniques. *Journal of Geotechnical and Geoenvironmental Engineering*, vol. 127, no. 8, pp. 688-698.

Matsuo, M.; Kuroda, K. (1974): Probabilistic approach to design of embankments. *Soils and Foundations*, vol. 14, no. 2, pp. 1-17.

Merifield, R. S.; Lyamin, A. V.; Sloan, S. W. (2006): Limit analysis solutions for the bearing capacity of rock masses using the generalised Hoek-Brown criterion. *International Journal of Rock Mechanics and Mining Sciences*, vol. 43, no. 6, pp. 920-937.

Oguz, E. A.; Yalcin, Y.; Huvaj, N. (2017): Probabilistic slope stability analyses: effects of the coefficient of variation and the cross-correlation of shear strength parameters. *Geotechnical Frontiers*, no. 278, pp. 363-371.

Pan, Q.; Xu, J.; Dias, D. (2017): Three-dimensional stability of a slope subjected to seepage forces. *International Journal of Geomechanics*, vol. 17, no. 8.

Park, H. J.; West, T. R.; Woo, I. (2005): Probabilistic analysis of rock slope stability and random properties of discontinuity parameters, Interstate Highway 40, Western North Carolina, USA. *Engineering Geology*, vol. 79, no. 3-4, pp. 230-250.

Phoon, K. K.; Kulhawy, F. H. (1999): Characterization of geotechnical variability. *Canadian Geotechnical Journal*, vol. 36, no. 4, pp.612-624.

Phoon, K. K.; Kulhawy, F. H. (1999): Evaluation of geotechnical property variability. *Canadian Geotechnical Journal*, vol. 36, no. 4, pp. 625-639.

Rocscience Inc. (2018): Slide2 version 2018 8.021-2D limit equilibrium slope stability analysis. http://www.rocscience.com.

Shen, J.; Karakus, M. (2013): Three-dimensional numerical analysis for rock slope stability using shear strength reduction method. *Canadian Geotechnical Journal*, vol. 51, no. 2, pp. 164-172.

Sun, H. Y.; Zhao, Y.; Shang, Y. Q.; Yu, Y.; Zhao, Q. L. (2012): Deep-seated slope failures induced by inappropriate cutting in China. *Rock Mechanics and Rock Engineering*, vol. 45, no. 6, pp. 1103-1111.

Tang, W. H.; Yucemen, M. S.; Ang, A. S. (1976): Probability-based short-term design of soil slopes. *Canadian Geotechnical Journal*, vol. 13, no. 3, pp. 201-215.

Viratjandr, C.; Michalowski, R. L. (2006): Limit analysis of submerged slopes subjected to water drawdown. *Canadian Geotechnical Journal*, vol. 43, no. 8, pp. 802-814.

Xiao, S.; Guo, W. D.; Zeng, J. (2017): Factor of safety of slope stability from deformation energy. *Canadian Geotechnical Journal*, vol. 55, no. 2, pp. 296-302.

Yang, X. L.; Pan, Q. J. (2015): Three dimensional seismic and static stability of rock slopes. *Geomechanics and Engineering*, vol. 8, no. 1, pp. 97-111.

Zhang, J.; Wang, H.; Huang, H. W.; Chen, L. H. (2017): System reliability analysis of soil slopes stabilized with piles. *Engineering Geology*, vol. 229, pp. 45-52.

Zhang, W. G.; Goh, A. T. C. (2013): Multivariate adaptive regression splines for analysis of geotechnical engineering systems. *Computers and Geotechnics*, vol. 48, pp. 82-95.

Zhang, W. G.; Goh, A. T. C. (2016): Multivariate adaptive regression splines and neural network models for prediction of pile drivability. *Geoscience Frontiers*, vol. 7, no. 1, pp. 45-52.

Zhang, W. G.; Goh, A. T. C. (2018): Reliability analysis of geotechnical infrastructures: introduction. *Geoscience Frontiers*, vol. 9, no. 6, pp. 1595-1596.

Zhang, W. G.; Goh, A. T. C.; Zhang, Y. M; Chen, Y. M; Xiao, Y. (2015): Assessment of soil liquefaction based on capacity energy concept and multivariate adaptive regression splines. *Engineering Geology*, vol. 188, pp. 29-37.

Zhang, W. G.; Zhang, Y. M.; Goh, A. T. C. (2017): Multivariate adaptive regression splines for inverse analysis of soil and wall properties in braced excavation. *Tunnelling and Underground Space Technology*, vol. 64, pp. 24-33.

Zhang, W. G.; Zhang, R. H.; Wang, W.; Zhang, F.; Goh, A. T. C. (2019): A multivariate adaptive regression splines model for determining horizontal wall deflection envelope for braced excavations in clays. *Tunneling and Underground Space Technology*, vol. 84, pp. 461-471.

Zhao, Y.; Tong, Z. Y.; Lü, Q. (2014): Slope stability analysis using slice-wise factor of safety. *Mathematical Problems in Engineering*, vol. 2014.

Zhou, S. L.; Liu, X. Q.; Shang, M. F.; Li, Y. (2012): Time-varying stability analysis of

mudstone reservoir bank based on water-rock interaction. *Rock and Soil Mechanics*, vol. 33, no. 7, pp. 1933-1939.

Zhou, S.; Rabczuk, T.; Zhuang, X. (2018): Phase field modeling of quasi-static and dynamic crack propagation: COMSOL implementation and case studies. *Advances in Engineering Software*, vol. 122, pp. 31-49.

Zhou, S.; Zhuang, X.; Rabczuk, T. (2018): A phase-field modeling approach of fracture propagation in poroelastic media. *Engineering Geology*, vol. 240, pp. 189-203.

Zhou, S.; Zhuang, X.; Rabczuk, T. (2019): Phase-field modeling of fluid-driven dynamic cracking in porous media. *Computer Methods in Applied Mechanics and Engineering*, vol. 350, pp. 169-198.

Zhou, S.; Zhuang, X.; Zhu, H.; Rabczuk, T. (2018): Phase field modelling of crack propagation, branching and coalescence in rocks. *Theoretical and Applied Fracture Mechanics*, vol. 96, pp. 174-192.